공학석사학위논문

Microrheology assays to study gelation of circular DNA by TOP2 clamp formation

원형 DNA와 TOP2의 젤 형성에 대한 미세유변학적 해석

2012년 8월

서울대학교 대학원

화학생물공학부

김연수

Microrheology assays to study gelation of circular DNA by TOP2 clamp formation

원형 DNA와 TOP2의 젤 형성에 대한
미세유변학적 해석

지도교수 **안 경 현**

이 논문을 공학석사학위논문으로 제출함
2012년 6월

서울대학교 대학원
화학생물공학부
김 연 수

김연수의 석사학위논문을 인준함
2012년 6월

위 원 장 _____

부위원장 _____

위 원 _____

Abstract

Microrheology assays to study gelation of circular DNA by TOP2 clamp formation

Kim, Yun Soo
School of Chemical and Biological Engineering
The Graduate School
Seoul National University

Topoisomerase II (TOP2) regulates DNA entanglement in replication, transcription, and repair. Driven by the hydrolysis of ATP, TOP2 has the ability to grab two strands of DNA and transpose their positions via a cleavage mediated passage reaction. TOP2 is a target for cancer therapeutics, because it is involved in late stages of cell division.

In this study, how generic TOP2 inhibitors affect the rheology of a model circular DNA solution was investigated by the microrheology gelation assays. The sol-gel transition of DNA-TOP2 was examined by using multiple particle tracking. By the time-cure superposition the gel kinetics of DNA and TOP2 was analyzed very accurately.

Inhibition of TOP2 was examined by the model inhibitor AMP-PNP and the anticancer drug ICRF-193. By using AMP-PNP rather than ATP, a closed clamp was formed by inhibiting the double strand passage reaction of TOP2. The result showed that both critical relaxation exponents and gel times decreased with increasing TOP2 concentration.

The change in double strand passage reaction was also examined while increasing ICRF-193 concentration under the presence of ATP. When ICRF-193 was bound to the ATP binding site of TOP2 the catalytic cycle was inhibited. Especially, when a sufficient amount of ICRF-193 was present, the gel formation characteristic was surprisingly similar to the case of AMP-PNP.

In this method, we have demonstrated that the microrheology method should be a novel assay to study many other anticancer drugs.

Keywords: microrheology, gelation, circular DNA, topoisomerase II, chemotherapy,
Student Number: 2009-23171

Contents

List of figures

List of tables

Chapter 1. Introduction

1.1. DNA Topoisomerase

The topological problems of disentangling DNA during different cellular activities are solved by an enzyme called topoisomerase . They catalyze the passage of a DNA strand through another. This reaction often results in the interconversion between the topological isomers of DNA rings and hence the name topoisomerase. DNA topoisomerase is of special interest due to their involvement in a large number of biological activities. They unlink DNA catenanes and resolve intertwined chromosomes and in their absence cause cell death (reviewed by Wang, 1998). They are also target for many anticancer drugs . These enzymes are also DNA-dependent ATPase. The binding and hydrolysis of ATP for the reaction to take place has been an area of fascinating research. In 1971, Wang discovered the first DNA topoisomerase in Escherichia−coli [1]. Gellert et al. in 1976 demonstrated that DNA gyrase catalyzed the formation of negative supercoils in double stranded DNA and this required the hydrolysis of ATP (reviewed by Chen and Liu). Liu et al. isolated T4 DNA topoisomerase in 1979 and showed that it catalyzed both negative and positive super coils. DNA topoisomerase acts by introducing a transient break in one of the DNA strands, holds it there, captures another strand by using ATP and allows it to pass through the broken strand by the hydrolysis of ATP [2-4]. The DNA enzymes are mainly classified into two categories based on the mechanism of action. They are the type I and the type II enzymes . Type I enzymes introduce transient single stranded breaks into DNA, pass an intact single strand of DNA through the broken strand and then re-ligate the break. Type II enzymes make transient double-stranded breaks into one segment of DNA

and pass an intact duplex through the broken double stranded DNA, before resealing the break [5, 6]. The type I enzymes include, bacterial DNA topoisomerase I and III, eukaryotic DNA topoisomerase III, eukaryotic DNA topoisomerase I and pox virus DNA topoisomerase IV. DNA type II topoisomerase II include topoisomerase IV, yeast and drosophilaDNA topoisomerase II, mammalian DNA topoisomerase IIα and IIβ and T-even phage DNA topoisomerase. In 1971, Wang proposed that DNA strand breaking occurs by a transesterification process.

1.2. Mechanism of action of DNA topoisomerase II

Topoisomerase II is a heart shaped dimeric protein with a large central hole of about 2-2.5 nm. The crystal structure of several type II topoisomerase has been determin. All the proteins possess an ATPase domain and DNA-binding domain. Pairs of like domains form dimer interfaces, which forms the gate for the passage of DNA. The DNA cleavage by topoisomerase II is a transesterification process between a pair of tyrosyl residues, present on each half of the dimeric enzyme, and a pair of DNA phosphodiester bonds separated by four base pair. The phenolic oxygen of the tyrosines of the enzymes become covalently linked with the phosphoryl groups of the 5’ ends of the transiently broken DNA leaving a pair of hydroxyl groups on the recessed 3’end of the DNA. The break is induced on both the strands of DNA separated by four base pairs. With the availability of ATP and another DNA double strand, the tyrosil-linked, 5’ ends of DNA moves apart while the base pairs between them are separated.

This opens a ’gate’ for the second double stranded DNA to pass through, after which the two strands are sealed back again.

Figure 1 shows the mechanism of the topoisomerase II catalytic cycle. It was proposed by Roca and Wang that topoisomerase act by an ATP modulated clamp. The reaction of the topoisomerase II begins when a double stranded DNA segment called the gate segment or the G-segment (because it forms a gate for the other DNA segment to pass through) binds to the two catalytic sites, the 5Y-CAP (catabolite gene activator protein) and the toprim, that forms the DNA gate. The second double stranded DNA segment called the transfer segment or T-segment is captured by the dimerisation of the ATPase domain, induced by two molecules of ATP. The hydrolysis of one molecule of ATP leads to the cleavage of the G-segment followed by the passage of the T-segment through the gate. The hydrolysis of the second ATP and the release of ADP leads to the opening of a third gate called the C gate, through which the T segment is passed out and the G segment is sealed back. This is followed by the opening of the ATP gate, and the enzyme is ready for the next cycle of reaction. Topoisomerase II requires two cofactors to carry out its catalytic doublestranded DNA passage reaction. First, it needs a divalent cation after the binding of the enzyme to DNA. Mg^{2+} is the divalent cation that the enzyme uses in vivo. This can be replaced by Mn^{2+} or Ca^{2+} ions in vitro. Second, topoisomerase II uses the energy of adenosine triphosphate (ATP) to drive the overall DNA strand passage reaction. The closing and opening of the ATP gate takes place regardless of the presence or absence of DNA. The binding of topoisomerase II to the DNA greatly stimulated the activity by about 20 folds. At low ATP concentration, about 2 ATP molecules are hydrolyzed during single DNA transport and at higher ATP concentrations, the transport

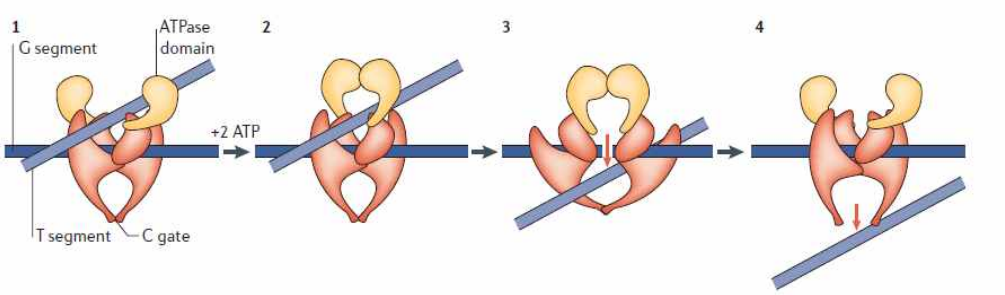

Figure 1.1 Mechanism of double strand passage by topoisomerase II

is less efficient as about 7 ATP molecules are utilized per DNA transport event.

1.3. Topoisomerase II inhibitors

The fact that DNA topoisomerase are target for therapeutic agents was discovered soon after the discovery of DNA gyrase. As seen in the previous sections topoisomerase II acts by breaking the double stranded DNA. These breaks introduced in the DNA strand are transient, i.e., they are short lived and within this time topoisomerase II does not cause any harm to the cells. However, any change in the conditions of the DNA-topoisomerase concentration leads to either inhibition of cell division or uncontrolled cell division. This uncontrolled growth of cells leads to cancer.

Topoisomerase II have been found to be the target of many anticancer drugs [7-18]. The mechanism by which anticancer drugs inhibit the action of topoisomerase II differ. It is known that they act by inhibiting at least one step of the catalytic cycle. Based on their action, the anticancer drugs are classified into two classes [14]. The agents that introduce a cytotoxic effect by stabilizing the covalent complex between DNA and topoisomerase II are called the cleavable complex [12, 13]. They introduce a double stranded break in the molecule leading to cell death and are referred to as topoisomerase poisons (classical inhibitors). Another important class of anticancer drugs act by inhibiting the activity of topoisomerase II at other stages of the catalytic cycle [11]. They do not introduce a double stranded break in the DNA molecule. They act by stabilizing the non covalent

complex. Hence they are referred to as catalytic inhibitors (non classical drugs) . Examples of catalytic inhibitors include merbarone, fostriecin, aclarubicin, suramin, bisdioxi-piperzines.

1.3.1. Adenylyl-imidodiphosphate (AMP-PNP)

Adenylyl imidodiphosphate is a non-hydrolyzable ATP. It is an inhibitor of ATP-dependent systems. AMP-PNP can bind to the topoisomerase II to lose the ATP domain and form an annulet. The closure of the jaws of the protein clamp is independent of the presence of the Tsegment of DNA . In such a conformation, the topoisomerase II can bind to linear molecules but not to circular molecules, as linear molecules can thread through the hole in the enzyme which is about 2 nm. The molecular structure of AMP-PNP is shown in Figure 1.1.

1.3.2. Bisdioxopiperazine (ICRF-193)

Bisdioxopiperazine derivatives belongs to a class of widely studied anticancer drugs. Several bisdioxopiperazine inhibit the action of topoisomerase II [10]. ICRF-154 is a frequently studied drug. They have been shown to stabilize the noncovalent complex formed between topoisomerase II and the DNA molecule and to hold the topoisomerase in a closed clamp position. ICRF-193, a dimethyl derivative of ICRF-154, has been shown to be most active towards topoisomerase II. Fattman et al. and Davies et al. have shown that topoisomerase IIα is sensitive to ICRF compounds suggesting that ICRF target topoisomerase II. Topoisomerase

IIα is shown to be ten times more sensitive to ICRF compared to topoisomerase II β.

Hu et al. has shown that the formation of non covalent complex requires both ATP as well as ICRF-193. It is still not well established if the topoisomerase II inhibition is due to the inhibition of topoisomerase II itself or due to the stabilization of the non covalent complex .

(a)

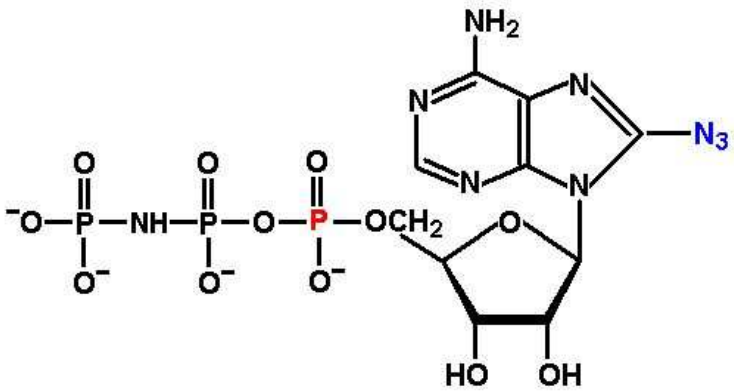

(b)

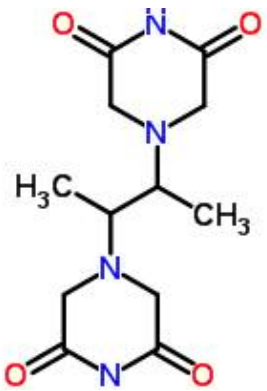

Figure 1.2 Molecular structure of Topoisomerase II inhibitors (a) AMP-PNP (b) ICRF-193

Chapter 2. Experimental

2.1. Materials

2.1.1 Topoisomerase II

Human topoisomerase II (TOP2) was purchased from Affymetrix. As supplied by the manufacturer, the TOP2 storage buffer contains 15 mM Na2HPO4, pH 7.1, 700 mM NaCl, 0.1 mM EDTA, 0.5 mM dithiothreitol (DTT), and 50% glycerol. The reaction buffer is composed of 10 mM TrisHCl, pH 7.9, 50 mM NaCl, 50 mM KCl, 5 mM MgCl2, 0.1 mM EDTA, and 15 mg/L bovine serum albumin. Adenosinetriphosphate (ATP), adenylylimidodiphosphate (AMPPNP), and meso4,4'-(3,2butanediyl)bis (2,6-piperazinedione) (ICRF193) ere purchased from SigmaAldrich.

2.1.2 λ DNA

λ DNA was purchased from New England Biolabs, Ipswich, MA. A 12 base long oligonucleotide with the complementary sequence of the right cohesive end of DNA, 5'AGGTCGCCGCCC3', was purchased from SigmaAldrich. The solution was concentrated to a concentration of 1.8 g of DNA/L by freeze drying and subsequently dialyzed in microdialyzers against TOP2 reaction buffer. The DNA concentration was determined by UV spectrometry. The stock solution was heated to 333 K, cooled to 295 K by immersion in a water bath, and the complimentary oligonucleotide was hybridized to one of the overhangs with a 100% excess molar ratios.

2.1.3 Cosmid

The cosmid (gift from Dr. C. Backendorf, Leiden University, The Netherlands), with a total size of 45 kbp, is derived from the Lawrist4 vector and contains a 40 kbp insert from the human chromosome 1q21 [19]. A colony of Escherichia Coli DH5 was transformed on a LB agar plate with kanamycin (50 mg/L). A single colony was taken to grow a culture in terrific broth (TB) medium (12 g of tryptone, 24 g of yeast extract, 4 mL of glycerol, 12.5 g of K2HPO4 and 2.3 g of KH2PO4 per L) and kanamycin (50 mg/L) at 310 K. After 6 h, this culture was put into flasks, which contained a total of 7.5 L TB medium and kynamycin. The bacteria were cultured for 19 h at 310 K under continuous shaking and, subsequently, harvested. The cells were suspended in TEG buffer (20 mM Tris, 10 mM EDTA, 50 mM glucose, pH 8.0) and lysed with an alkaline solution (1% SDS, 0.2 M NaOH). Bacterial genomic DNA, cellular debris, and proteins were precipitated by the addition of 4 M potassium acetate and 2 M acetic acid followed by incubation on ice. RNA and protein were removed with an RNAse (20 mg/L, 310 K, 12 h) treatment and phenol extraction, respectively. After precipitation with ethanol, the pellet was dried for a short time, suspended in TE buffer (10 mM TrisHCl, 0.1 mM EDTA, pH 8.5) and, eventually dialyzed against reaction buffer with a final concentration of 3.5 g of cosmid/L [30].

The integrity of the cosmid and λDNA was checked with pulsed field inversion. 1% agarose gel electrophoresis in TAE buffer (40 mM Trisacetate, 1 mM EDTA, pH 8.3) at 6 V/cm for 9 h. The gel image obtained by ethidium bromidestaining is shown in Fig. 7. In order to assign the different

bands in the chromatogram, we have treated the cosmid with TOP2 or restriction endonuclease NruI (New England Biolabs). After treatment with TOP2, closed circular, supercoiled cosmid is relaxed with linking number deficits $\Delta Lk = 0$ or 1. Circular cosmid is converted into a linear form by the endonuclease. The chromatogram of the cosmid preparation shows a weak band at 45 kbp, an intense band at a slightly lower migration distance of around 55 kbp, and a smear next to the loading reservoir. After treatment with TOP2, the intense band at around 55 kbp disappears. Concurrently, the intensity of the smear increases and there is no appreciable change in intensity of the weak band at 45 kbp. The linearized cosmid shows no smear and a single broad band around 45 kbp. From these results we conclude that the strong and weak bands at 55 and 45 kbp correspond with the cosmid in the tightly interwound supercoiled and linear form, respectively. The smear next to the loading reservoir comes from open circular DNA, branched supercoils, as well as DNA's with low degree of supercoiling. From the integrated band intensities we conclude that 5% of the cosmid is in the linear form. It is difficult to quantify the fractions of supercoiled and open circular cosmid, but at least 65% is tightly interwound. Furthermore, neither degradation nor multimerization of hybridized λ DNA was observed.

2.2 Sample preparation

Samples were prepared by dilution of the stock solution with reaction buffer. After dilution, but before the addition of the enzyme, all samples were equilibrated at least overnight. Three series of experiments were done. For the first series, solutions with concentrations of 0.7, 1.7, and 2.4 g of

cosmid/L were prepared. These solutions do not contain TOP2 and provide the blanks. In the second series, we investigated the effect of AMPPNP in conjunction with TOP2 on the properties of the flow. For this purpose, TOP2 was added to solutions of 1.6 g of cosmid/L in ratios of 2, 4, and 6 units per μg of DNA with an AMPPNP concentration of 2.5 mM. We also prepared a solution of 1.6 g of cosmid/L with 4 units of TOP2 per g of DNA and an ATP concentration of 2.5 mM. In the third series, TOP2 inhibition with ICRF193 is investigated. Here, TOP2 was added to solutions of 1.6 g of cosmid/L in ratios of 2 and 6 (1 mM ICRF193 only) units/g with an ATP concentration of 2.5 mM and ICRF193 concentrations of 0.1 and 1 mM, respectively. We have also investigated solutions of 1.0 g of λDNA g/L with 4 units/μg of TOP2. The latter solutions also contained 2.5 mM AMPPNP or 2.5 mM ATP and 1 mM ICRF193. One unit of TOP2 (20 ng) is the amount of enzyme required to fully relax 0.3 μg of negatively supercoiled pBR322 plasmid DNA in 15 minutes at 303 K in standard assay conditions. With a molecular weight of 340 kDa, one unit per g of cosmid

DNA (45 kbp) corresponds with 1.7 dimers per DNA molecule. All samples were spiked with polystyrene fluorescence microspheres (Bangs Laboratories, IN) of 1.90.2 μm diameter with a final concentration of 0.08 wt% . The microspheres are internally labeled with dragon green with a maximal excitation and emission wavelength of 480 and 520 nm, respectively. Just before the microrheology experiment, we added about 2 μL of the enzyme in storage buffer to 10 μL of DNA in reaction buffer, followed by mixing the solution for 20 s through gentle stirring and pipetting up and down. Shear was minimized by using pipette tips that have

wide openings. A droplet of solution was deposited on a microscopy slide and sealed with a coverslip separated by a 0.2 mm spacer. The slide is subsequently loaded on the preheated and temperature controlled stage of the microscope. All measurements were done at 310 K. All samples were assayed at least in duplicate. The initial time is taken as the time when the specimen was loaded on the preheated microscopy stage.

2.3 Microrheology

Particle tracking experiments [28] were carried out at 310 K with an inverted Olympus IX71 fluorescence microscope equipped with a 50X long working distance objective, numerical aperture of 0.35, and an ALPHA Vivid XF1003 filter set (Omega Optics, Brattleboro, VT). In order to minimize hydrodynamic interactions, the imaged beads are separated by at least 10 bead diameters (20μm). Furthermore, the focal plane was adjusted to be midway between glass slide and coverslip. Video was collected with an electron multiplying charge coupled device (EMCCD) camera (Andor iXon 897) and Andor Solis software. We have checked our setup by measuring the diffusion of colloidal beads dispersed in a concentrated solution of glycerol as well as by monitoring immobilized beads adsorbed at a glass slide. The tracking experiment was recorded with a rate of 107 frames per second, frame size of 128 x 128 pixels, and exposure time of 1 ms. The exposure time is short enough to minimize dynamic error and the static error in x^2, as estimated by monitoring immobilized beads, is around 10 nm^2 [29]. Each clip has a duration of 100 s and the total duration of the movie is 100 minutes. The clips were taken randomly in the xy plane and in

each clip the trajectories of 2 to 6 particles were recorded. The video was analyzed with matlab (Natick, MA) and the particle trajectories were obtained with public domain tracking software (http://physics.georgetown.edu/matlab/). All further data analysis was done with home developed software scripts written in matlab code.

2.4 Time-cure superposition

The MSD changing with gelation was analyzed by the time-cure superposition devised by Furst [33-36]. To minimize the arbitrariness of the problem in the process of time-cure superposition we have used the following method. We first found the local logarithmic slope from MSD and then we shifted the x- and y-axes to match the slopes smoothly. By this method we have tried to extract the intrinsic superposition without arbitrariness. The same logarithmic slope will be used when viscoelastic moduli is calculated so that the time-cure superposition and viscoelastic moduli should have the consistency. When logarithmic slope increased as function of lag time the pre-gel master curve was superposed. When the slope was constant, the time was defined as the gel point. When the slope decreases as function of lag time in the later stage post gel master curve was constructed. In the case of pregel, however, the logarithmic slope did not decrease monotonically and therefore it was impossible to avoid arbitrariness completely. In this case we tried to fit to the best superposition. We plot two shift factors a and b as a function of gelation time and monitored the gelation kinetics, where a and b represent the lag time shift factor and MSD shift factor, respectively.

Chapter 3. Results

3.1 Viscoelastic properties of cosmid solution

Figure 3.1. shows the ensemble-averaged MSDs as a function of time, τ, for different DNA concentrations. With increasing DNA concentration, the mean square displacement decreases.

The MSD of 0.7 mg/mL of cosmid is a straight line in the logarithmic representation meaning that it is a viscous fluid. For the cosmid concentration of 1.2 and 1.6 mg/mL, the graph begins to deviate from the linear behavior at an intermediate frequency. At short delta t, we can see a subdiffusive scaling exponent less than one. The deviation from linear behavior for short τ is due to the viscoelastic behaviour of DNA solution [32]. Throughout the whole experiment set with addition of TOP2 the DNA concentration is fixed at 1.67mg/mL. The initial state is viscoelastic fluid as shown in the graph.

The catalytic cycle of TOP2 requires ATP. When ATP is replaced by AMP-PNP, the protein can close and form a clamp.

Adenylyl-imidodiphosphate (AMP-PNP), unhydrolysable form of ATP, is a generic topo II inhibitor. It binds to TOP2 in the same fashion as ATP, but it cannot be hydrolyzed. Triggered by the binding of AMP-PNP, the protein dimer closes, cannot be re-opened, and is converted to a closed clamp. Here, we explore the effect of topology on the DNA flow property. For this purpose, we have added 4units of TOP2 per ug of DNA (about 8 dimers per DNA molecule) to λ DNA and cosmid solutions respectively and monitored the trajectories of the probe beads as a function of the time evolved after the addition of the enzyme. Note that the two DNAs have almost the same molecular weight. (50kbp for cosmid, 48.5kbp for λ DNA)

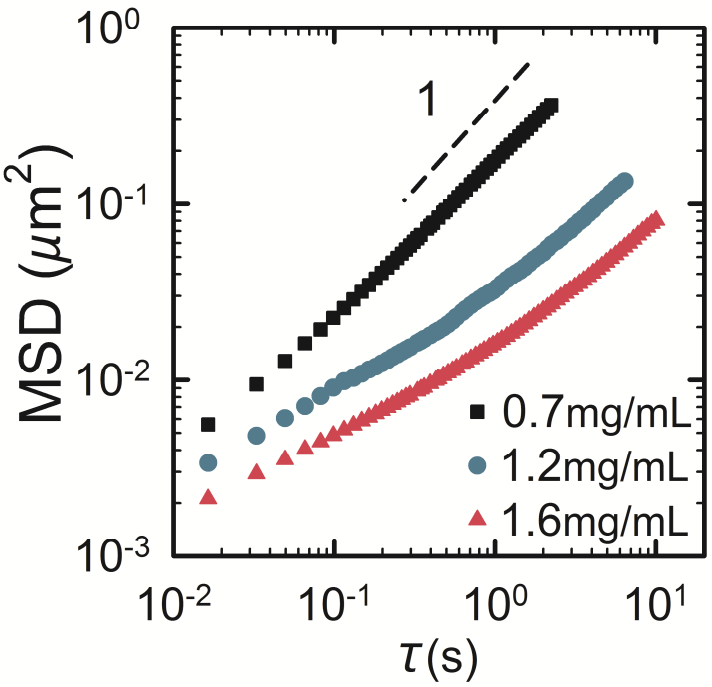

Figure 3.1 (a) The ensemble-averaged mean square displacement <Δx2(t)> as a function of lag time τ for cosmid concentrations of 0.7 mg/mL (■), 1.2 mg/mL (o) and 1.6 mg/mL (Δ).

3.2 The role of DNA topology on gel formation

To follow the kinetics, the evolution of the MSD evaluated at a given lag time is represented with the reaction progression. In figure 3.2, we plot the normalized MSD, calculated at lag time τ=1s as a function of reaction time. We normalized the MSD with the initial MSD value to compare two cases from the same level.

In the case of λ DNA, normalized MSD is seen to decrease followed by an increase towards the original entangled state. The constraints are transient and short-lived, due to the threading motion of the linear DNA molecule through the hole of the clamp [5-7]. Accordingly, for the case of λ DNA, we do not observe the fixed cross-links [37]. However, the situation is different for closed circular DNA. The MSD decreases towards a plateau values as time passes. This is because a captured circle cannot be released by threading motion. Since there are no free ends in cosmid, it cannot reptate out of the clamp. For these reasons, it forms a permanent crosslink as we propose in figure 2(b).

As described above the viscoelastic property changes dramatically with the topology of DNA. In the next studies we have investigated whether circular DNA's can form a gel ultimately.

(a)

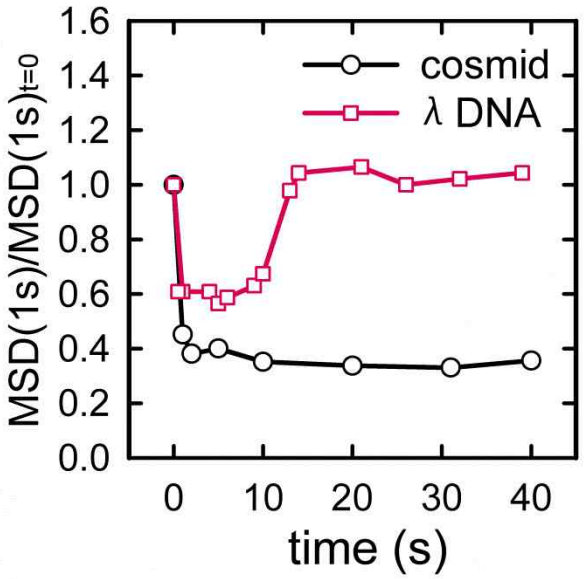

(b)

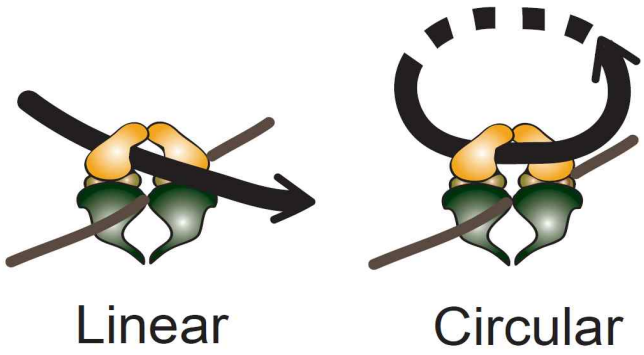

Figure 3.2 (a) Normalized MSD at τ=1s versus time, t, after the addition of topoisomerase II (4 units/μg) to a solution of 1.0 mg/ml of λ-DNA (□) and 1.67 mg/ml (○) of Cosmid in 2.5mM AMP-PNP (b) Comparison between λ-DNA and Cosmid

3.3 Inhibition of topoisomerase II with AMP-PNP

3.3.1. Time-cure superposition

The gelation kinetics are analyzed by time-cure superposition of the tracer particle mean square displacement.

In exploring the questions of gelation, we will limit ourselves to consideration of circular DNA. In order to verify the effect of the concentration of TOP2 on flow property, experiments were performed with different TOP2 concentrations; from 1 to 6 units per ug of DNA (2 and 12 dimers per DNA molecule). The DNA concentration was fixed at 1.67 mg/mL. After the addition of TOP2, we monitored the MSD for 100minutes. Adolf and Martin first demonstrated time-cure superposition using bulk rheology data taken at various extent of reaction for epoxy [31]. As the reaction time increases, the shape or structure of the network does not change, only the length scale and corresponding relaxation time is changed. This is the underlying principle as well as the reason for the time-cure superposition.

As the system approaches the gel-point, the shape of the MSD is invariant but the curve shifts upwards and to the right and the length scales and time scales increase. Around the gel-point, many networks are self-similar and show the fractal nature of structure. The postgel MSD, which curves towards a plateau at large τ, then shifts downwards and to the left as the network matures and the mesh size decreases. Thus, following the method of Larsen & Furst [30], the MSDs can be superposed to form two mastercurves, pregel and postgel by applying horizontal, a and vertical, b

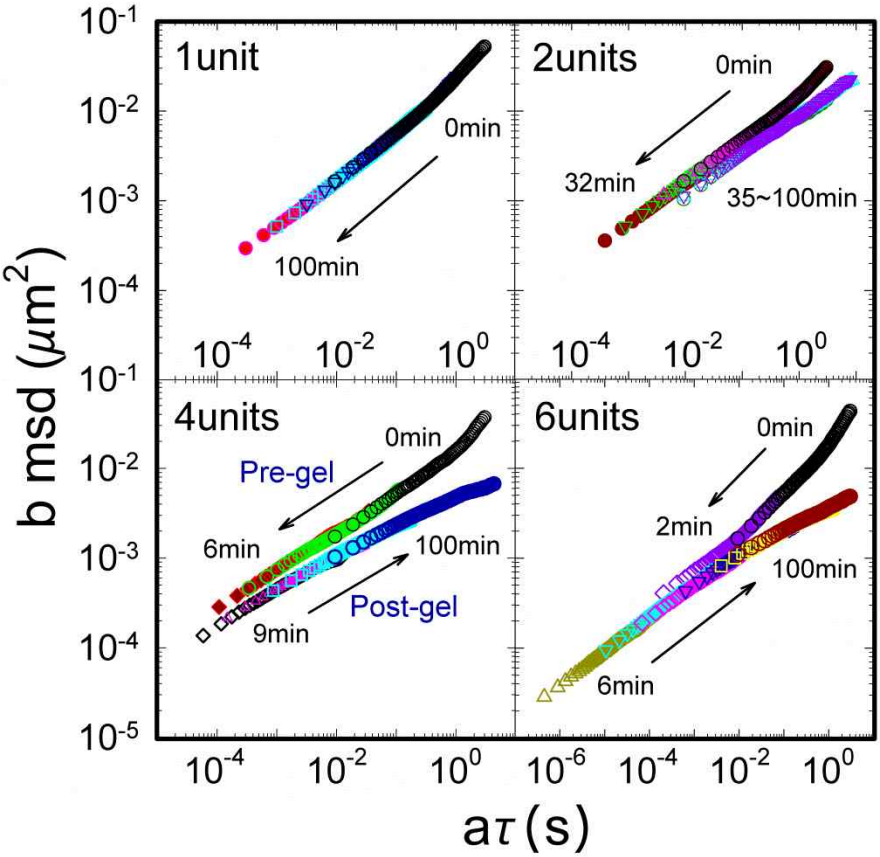

Figure 3.3 Gelation kinetics with different TOP2 concentrations in 2.5mM AMP-PNP analyzed by time-cure superposition. The mean-squared displacements are shifted into pre- and post-gel master curves.

shifts to each curve. This has been performed for the each set of MSDs in Figure 3.3.

After the addition of TOP2, the local structure keeps growing as DNA is cross-linked by TOP2. With the cross-linking of DNA, the curves shift downwards as the viscosity slowly increases. The logarithmic gradient begins to decrease at short lag times. This corresponds to small clusters relaxing at short lag times and diffusing over long lag times.

As the size of the clusters increase, the characteristic relaxation times increase until the MSD is subdiffusive (the logarithmic gradient is less than 1) over all lag times and a single, self-connected network is formed. This fractal network-forming time is defined as the gel point. At the gel point the MSD shows the power law and the slope value "n" is called the critical exponent. After this gel point, the MSD curves downwards towards a plateau instead of upwards towards diffusive behavior, meaning that an elastic network has formed. As the gelation time, t, increases, both the height of the plateau and the lag time, τ, at which it develops decrease as the mesh size and characteristic relaxation times decrease.

For the 1 unit of TOP2, at the end of the reaction it is still viscoelastic since it is before fully crosslinked. Therefore only pre-gel mastercurve was constructed. The resulting pregel master curve has logarithmic slope 1 at long lag times $a\tau$, which decrease monotonically with decreasing $a\tau$. However, With 2 units of TOP2 the msd curve collapses into one cuve for the first 32 min since the start of the reaction and collapses to another curve after 35 min. The all the msds after 35min follow a power law behavior slope of 0.44, which shows that 2 units is critical TOP2 gelation concentration. For 4units and 6units, we get two distinct curves which are the clear evidences of gel formation and the critical exponent at gel point is

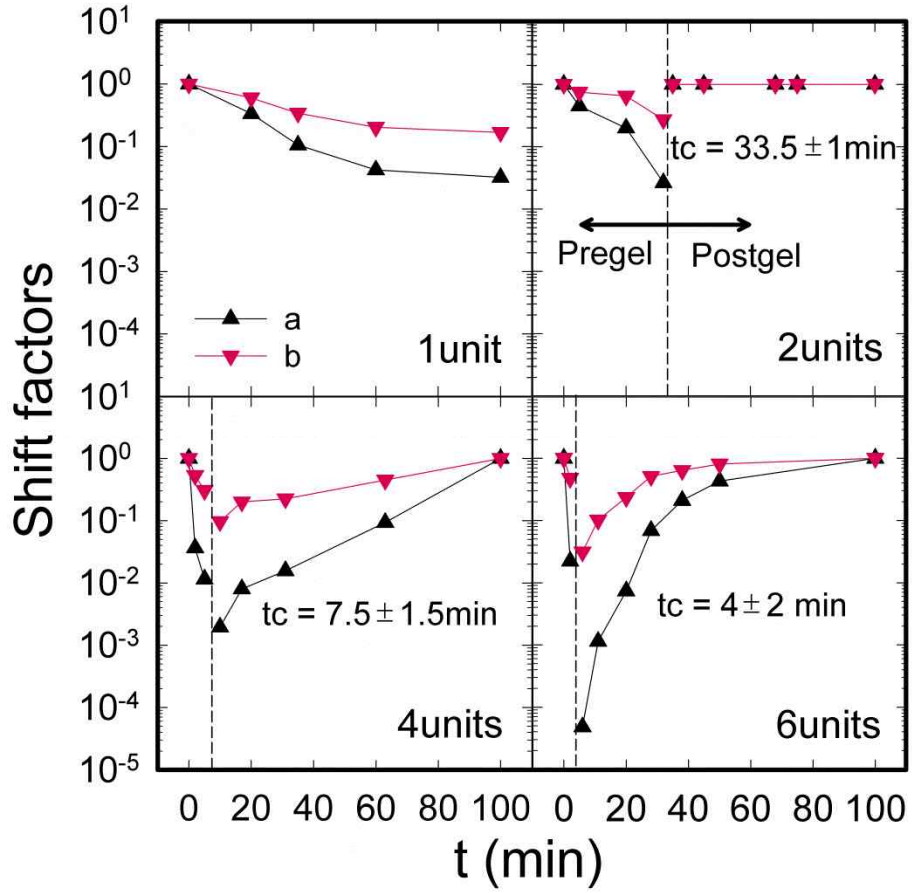

Figure 3.4 Lag time shift factor a(Δ), MSD shift factor b(∇) used for superposition in figure 3

0.40 and 0.35 respectively.

Overall, critical exponents, n decreases as increasing TOP2 concentration within the error range as shown in Table 1. This agrees with the classical polymer gelation by crosslinker. Winter shows that the critical exponent is decreased as cross linker concentration increasing [25].

3.3.2. Gelation kinetics

Fig.3.4 shows the plot of Lag time shift factor a(Δ), MSD shift factor b(▽) as a function of time, t, for the different TOP2 concentrations in 2.5mM AMP-PNP. The critical gel point, tc is denoted by the dashed vertical line.

The lag time shift factor, a, is inversely proportional to the longest relaxation time in the system, and the MSD shift factor, b, is inversely proportional to the steady-state creep compliance, J0, both of which diverge around the gel-point. We plot the shift factors as a function of time from which the gel kinetics can be easily determined.

With 1 unit of TOP2, both a and b gradually decreases. In the case of 2unit, shift factors after 35 min are both 1 and these values do not change until the reaction is completed. This implies that this is the critical TOP2 concentration in the formation of gel hence cross-linking reaction stops exactly at gel point, due to the deficiency of the cross-linker.

It should be noted that there is no shift factor at the gel point. This is because the shift factor b is the inverse of the creep compliance.

As described above, both critical relaxation exponents and gel times are decreased with increasing TOP2 concentration, showing that the inhibited enzyme acts as a gelator.

3.3.3. Dynamic scaling exponents

The values of the critical exponents determined above are based on the assumption that the gel-time has been calculated accurately. It is therefore useful to have a method of calculate the critical exponent, n, which is independent of the choice of gel-time. This can be done by plotting the shift factors, a and b against each other. To do this, we use the relationship $a \propto \varepsilon^{y}$ and $b \propto \varepsilon^{z}$, $b \propto a^{z/y} \propto$ an equation, where $\varepsilon = |t-tg|/tg$ is the distance from the gel point and y, z are the dynamic scaling exponents. The shift factor follows power law, the value obtained from the logarithmic slope of MSD at the gel point. This power law behavior is observed for the whole range of gelation times, and n is in excellent agreement with the value found from MSD .The n values were in agreement for 2~6 unit which form gels and the agreement was better for postgels rather than pregels) This is strong evidence that the gel time, and the resulting critical exponent are reliable.

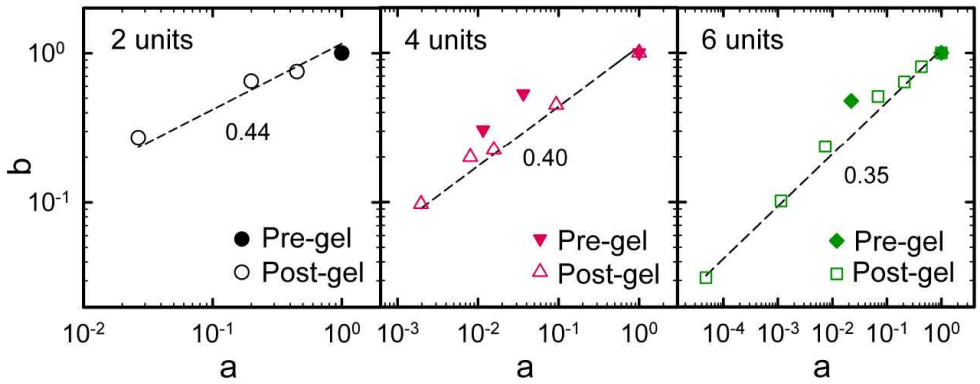

Figure 3.5 Dynamic scaling exponents obtained from the relationship between shift factor a and b used for pre-gel (open symbols) and post-gel (closed symbols) master curve.

Dashed lines indicate the corresponding critical relaxation exponent of different TOP2 concentrations calculated from MSD; 0.44 for 2units (●), 0.40 for 4units (Δ), and 0.35 for 6units (□).

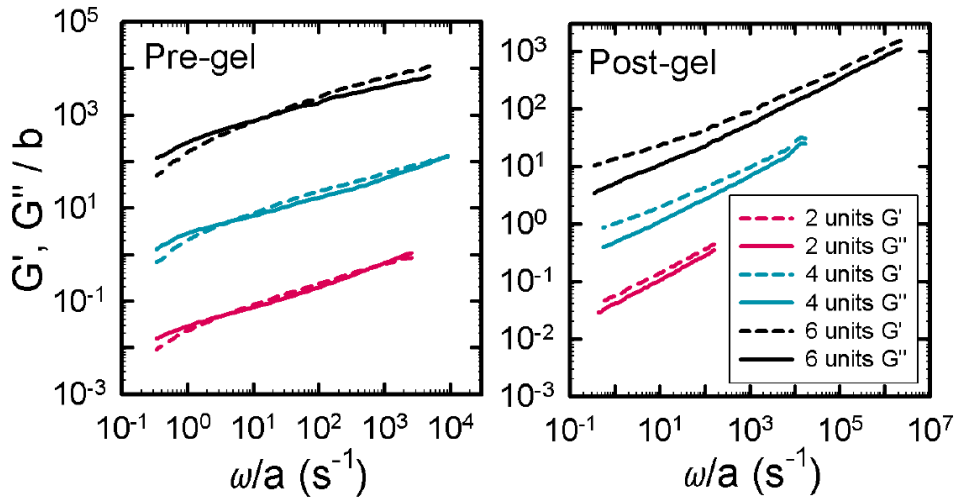

Figure 3.6 G', G'' superposition using pregel and post gel mastercurves. (a) G',G'' superposition

3.3.3. Viscoelastic moduli superposition

Adapting Fourier transform of the MSD to calculate the viscoelastic modulid can introuduce truncation errors due to the finite nature of MSD data. The size of the error varies depending on the method of transform used, but in general becomes significant near the extreme of frequency. However, the method of superposition of MSDs creates master curves for the pregel and postgel that are reliable over ~7 orders of magnitude. This allow the moduli to be found over a similarly wide frequency range for all reaction times; only the scaling of the modulus and frequency changes as the gelation proceeds.

At the gel point G' and G" show power laws and the power law exponent n coincides with the critical exponent of MSD. When G' and G" were superimposed it was found that the pregel master curves showed a typical viscoelastic behavior of crossing G' and G" while the postgel curves showed a typical gel-like behavior. Especially in the case of pregel curves, the accessible region of the frequency spectrum shifts toward higher region as TOP2 concentration increases.

3.4 Inhibition of topoisomerase II with ICRF- 193

3.4.1. Time-cure superposition

In this case we performed an inhibition of TOP2 by using ICRF-193 rather than AMP. In the experiments with ICRF-193, a DNA solution of 1.67 mg/mL was prepared with an ATP concentration of 2.5 mM and a series of

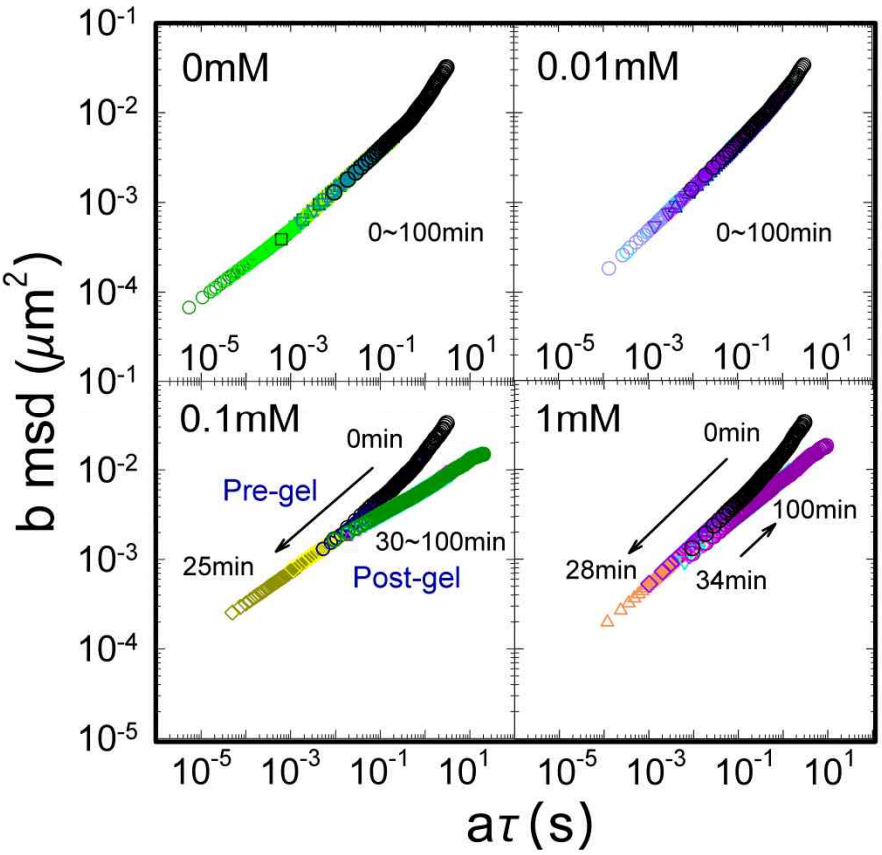

Figure 3.7 Gelation kinetics with different ICRF-193 concentrations in 2.5mM ATP analyzed by time-cure superposition. The mean-squared displacements are shifted into pre- and post-gel master curves.

different ICRF-193 concentration. 2 units of topoII per micro gram of DNA were added to the solutions and the experiments were performed at 310 K. The time-cure superposition of MSD after the addition of TOP2 is shown in Figure 3.7. For 0mM and and 0.01mM only the pregel master curves were constructed. However for higher concentration, 0.1mM and 1mM, we found that the postgel master curves are constructed as well, and it is very similar to the case of AMP-PNP 2 units. Since the double strand passage activity is suppressed by binding ICRF-193, a cross-linking protein clamp between two DNA segments is formed, just like in the case of AMP-PNP. The gel kinetics were analyzed by plotting shift factors in figure 8.

In the absence of ICRF-193, double-strand passage reaction proceeds and it is successfully characterized by time-cure superposition. The shift factors are seen to decrease immediately after the addition of the enzyme. This indicates that supercoils are relaxed at the beginning. Then it is increases due to the relaxing the entanglement followed by a recovery to the entangled state [34].

In the presence of a 0.01M ICRF-193, the trend is similar but the magnitude is reduced compare to the case of 0mM of ICRF-193. It is evident from this observation that ICRF-193-193 inhibits the activity of TOP2. Hence, the double-strand passage reaction gets progressively blocked, so that increasingly fewer reactions were proceed.

After adding sufficient amount of ICRF-193, the trend is significantly changed. From the stoichiometric viewpoint ICRF-193 was added in far excess since each topo corresponds to ICRF-193.

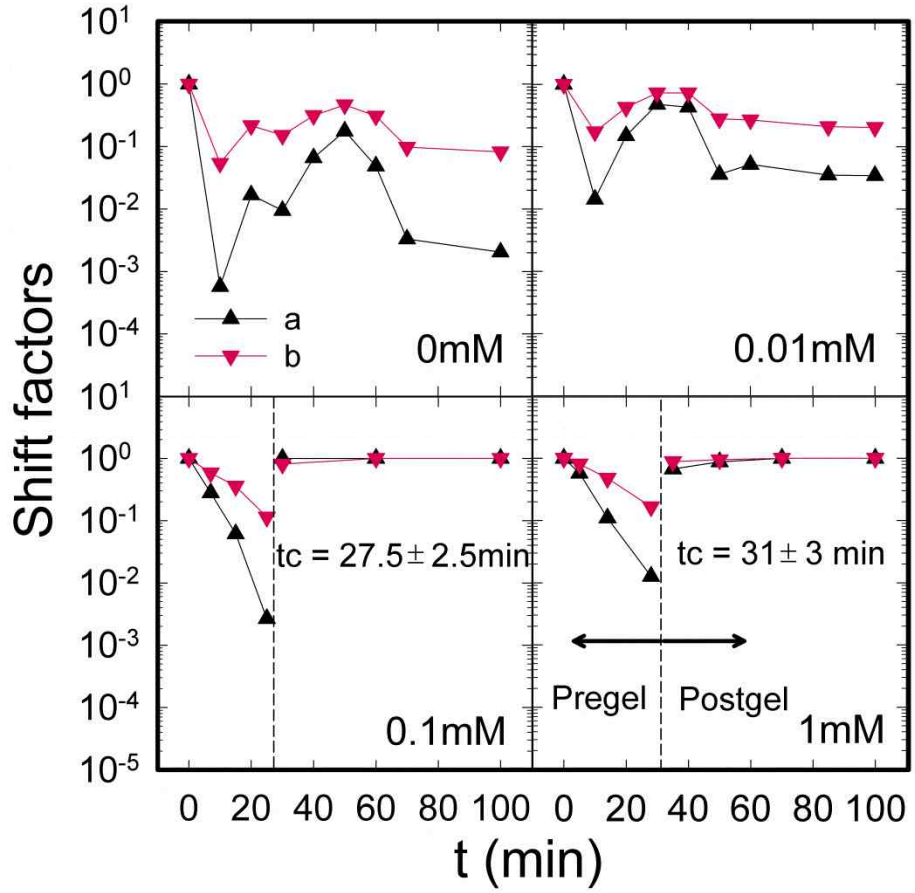

Fig. 3.8 Lag time shift factor a(Δ), MSD shift factor b(∇) with 2units of topoisomerase II in 2.5mM ATP, 2.5mM AMP-PNP and 2.5mM ATP with 1mM ICRF-193-193 (from left to right).

3.4.2. Gelation kinetics

The shapes of pre- and post-gel master curves were very similar to the case of AMP-PNP 2 units of TOP2. Also the critical exponent and gel time were similar to the cases of AMP-PNP. It is plausible that the slight difference is due to the relaxation of DNA supercoils before the ICRF-193 combines with topo. This means that the ICRF-193 effectively inhibits TOP2 by the similar mechanism to AMP-PNP.

Since Roca reported that ICRF-193 inhibited TOP2 in 1994 [10], there have been many researches on this topic. Morris argued that ATP should be hydrolyzed slowly even though ICRF-193 is bound to topo [17]. But in the present research we have found that the hydrolysis of ATP is negligible when the amount of ICRF-193 is sufficiently large.

In 2008 Roca presented an interesting hypothesis on ICRF-193 [15]: A hypothesis on C-gate padlock as well as N-gate. To confirm the hypothesis, an extreme condition has to be given. It may not be reasonable in that the residence time of t-segment should be extremely long to show that c-gate padlock is required in cross-linking. In the present research we have observed that the gel-kinetics of the case of ICRF-193 is very similar to the case of AMP-PNP. This implies that cross-linking should be possible without C-gate padlock. Then one may suspect the mechanism of ICRF-193 proposed until now. They argue that the the bisdioxopiperazine class of drugs such as ICRF-197 and 193 has a function on the last step of the catalytic cycle: The hydrolysis and release of ADP+P causes the disassociation of the ATPase domain and the opening of the N-terminal gate to allow the release of the G-segment and the return of topoII to its native state. However, it may not be the case based on the our observation.

Huang reported that both cross-linking and DNA cleavage occurred when ICRF-193 is added [9]. Hajji also reported the breakage of DNA strands [8]. In the present research, however, we have not been able to observe the destruction of gel-like structure even when the flow property was investigated for a sufficiently long gelation time of 100 mins. Since the TOP2 is covalently bound to the DNA, we couldn't conclude the DNA breakage although there was no gel destruction in reaction time.

Until now we have found that DNA is gelled by the inhibition of TOP2 by ICRF-193 and proved that the mechanism of this process is very similar to the case of AMP-PNP. We may consider another possibility in the process of cross-linking: The catenation of DNA by the double strand reaction of DNA before the binding of ICRF-193 [35]. However this appears to be a minor factor and, even if this is true, the control of DNA flow property, in other words, the gelation of DNA should be of significant meaning.

It should be an interesting experiment to confirm whether DNA would have a flow-like behavior when TOP2 is removed by using protainase K.

Cosmid	ATP/AMP-PNP	TOP2	ICRF-193	n	tc
1.67mg/ml	AMP-PNP	1unit	-	-	-
		2units	-	0.44	34±1min
		4units	-	0.40	8±2min
		6units	-	0.35	4±2min
	ATP	2units	0mM	-	-
		2units	0.01mM	-	-
		2units	0.1mM	0.39	28±3min
		2units	1mM	0.42	31±3min

Table 1 Critical relaxation exponents and critical gel time obtained by power-law behavior of MSD at the gel point

Chapter 4. Conclusion

In summary we have investigated DNA flow properties by the microrheology gelation assay. By using AMP rather than ATP, a closed clamp was formed by inhibiting the double strand passage reaction of TOP2. First of all the change in flow properties was investigated depending on topology difference. The effect of topology on flow properties was examined by comparing linear and circular DNAs. In the case of linear DNA, TOP2 and DNA formed a dynamic and short-lived structure and then the DNA moved out through the clamp hole while the circular DNA could not move out through the hole since it did not have a free ends and hence a stable fixed clamp was formed.

Next we examined the gel kinetics of circular DNA while increasing the amount of crosslinker, TOP2. The result showed that both critical relaxation exponents and gel times decreased with increasing TOP2 concentration when the gelation was analyzed by the time-cure superposition.

Then topo was inhibited by ICRF-193. The change in double strand passage reaction was examined while increasing ICRF-193 concentration under the presence of ATP. The result showed that the catalytic cycle of TOP2 proceeded with the hydrolyzation of ATP when there was no ICRF-193. When ICRF-193 was bound to the ATP binding site of TOP2 the catalytic cycle was inhibited. Especially, when a sufficient amount of ICRF-193 was present, the gel formation characteristic was surprisingly similar to the case of AMP-PNP.

In conclusion, we have demonstrated that the microrheology method should be a novel assay to study many other anticancer drugs.

References

1. James C, W., *Interaction between DNA and an Escherichia coli protein ω.* Journal of Molecular Biology, 1971. **55**(3): p. 523-IN16.
2. Nitiss, J.L., *DNA topoisomerase II and its growing repertoire of biological functions.* Nat Rev Cancer, 2009. **9**(5): p. 327-337.
3. Duplantier, B., G. Jannink, and J.L. Sikorav, *Anaphase chromatid motion: involvement of type II DNA topoisomerases.* Biophysical journal, 1995. **69**(4): p. 1596-1605.
4. Sikorav, J.L. and G. Jannink, *Kinetics of chromosome condensation in the presence of topoisomerases: a phantom chain model.* Biophysical journal, 1994. **66**(3, Part 1): p. 827-837.
5. WANG, J.C., *Moving one DNA double helix through another by a type II DNA topoisomerase: the story of a simple molecular machine.* Quarterly Reviews of Biophysics, 1998. **31**(02): p. 107-144.
6. Berger, J.M., et al., *Structure and mechanism of DNA topoisomerase II.* Nature, 1996. **379**(6562): p. 225-232.
7. Roca, J. and J.C. Wang, *The capture of a DNA double helix by an ATP-dependent protein clamp: A key step in DNA transport by type II DNA topoisomerases.* Cell, 1992. **71**(5): p. 833-840.
8. Hajji, N., et al., *DNA strand breaks induced by the anti-topoisomerase II bis-dioxopiperazine ICRF-193.* Mutation Research/Fundamental and Molecular Mechanisms of Mutagenesis, 2003. **530**(1-2): p. 35-46.
9. Huang, K.-C., et al., *Topoisomerase II Poisoning by ICRF-193.* Journal of Biological Chemistry, 2001. **276**(48): p. 44488-44494.
10. Roca, J., et al., *Antitumor Bisdioxopiperazines Inhibit Yeast DNA Topoisomerase II by Trapping the Enzyme in the Form of a Closed Protein Clamp.* Proceedings of the National Academy of Sciences of the United States of America, 1994. **91**(5): p. 1781-1785.

11. Andoh, T. and R. Ishida, *Catalytic inhibitors of DNA topoisomerase II.* Biochimica et Biophysica Acta (BBA)/Gene Structure and Expression, 1998. **1400**(1): p. 155-171.
12. Froelich-Ammon, S.J. and N. Osheroff, *Topoisomerase Poisons: Harnessing the Dark Side of Enzyme Mechanism.* Journal of Biological Chemistry, 1995. **270**(37): p. 21429-21432.
13. Chen, A.Y. and L.F. Liu, *DNA topoisomerases: essential enzymes and lethal targets.* Annual review of pharmacology and toxicology, 1994. **34**(1): p. 191-218.
14. Nitiss, J.L. and W.T. Beck, *Antitopoisomerase drug action and resistance.* European journal of cancer (Oxford, England : 1990), 1996. **32A**(6): p. 958-66.
15. Roca, J., *Topoisomerase II: a fitted mechanism for the chromatin landscape.* Nucleic Acids Research, 2009. **37**(3): p. 721-730.
16. Proceedings of the National Academy of Sciences, 2003. **100**(24): p. 14510.
17. Morris, S.K., C.L. Baird, and J.E. Lindsley, *Steady-state and Rapid Kinetic Analysis of Topoisomerase II Trapped as the Closed-clamp Intermediate by ICRF-193.* Journal of Biological Chemistry, 2000. **275**(4): p. 2613-2618.
18. Hu, T., H. Sage, and T.-s. Hsieh, *ATPase Domain of Eukaryotic DNA Topoisomerase II.* Journal of Biological Chemistry, 2002. **277**(8): p. 5944-5951.
19. Cabral, A., et al., *Structural Organization and Regulation of the Small Proline-rich Family of Cornified Envelope Precursors Suggest a Role in Adaptive Barrier Function.* Journal of Biological Chemistry, 2001. **276**(22): p. 19231-19237.
20. Quertermous, T., *Purification of Bacteriophage Clones*, in *Current Protocols in Molecular Biology*2001, John Wiley & Sons, Inc.

21. Robertson, R.M., S. Laib, and D.E. Smith, *Diffusion of isolated DNA molecules: Dependence on length and topology.* Proceedings of the National Academy of Sciences, 2006. **103**(19): p. 7310-7314.
22. Robertson, R.M. and D.E. Smith, *Self-Diffusion of Entangled Linear and Circular DNA Molecules: Dependence on Length and Concentration.* Macromolecules, 2007. **40**(9): p. 3373-3377.
23. Robertson, R.M. and D.E. Smith, *Strong effects of molecular topology on diffusion of entangled DNA molecules.* Proceedings of the National Academy of Sciences, 2007. **104**(12): p. 4824-4827.
24. Goodman, A., Y. Tseng, and D. Wirtz, *Effect of Length, Topology, and Concentration on the Microviscosity and Microheterogeneity of DNA Solutions.* Journal of Molecular Biology, 2002. **323**(2): p. 199-215.
25. Chambon, F. and H.H. Winter, *Linear Viscoelasticity at the Gel Point of a Crosslinking PDMS with Imbalanced Stoichiometry*. Vol. 31. 1987: SOR. 683-697.
26. Osheroff, N., E.R. Shelton, and D.L. Brutlag, *DNA topoisomerase II from Drosophila melanogaster. Relaxation of supercoiled DNA.* Journal of Biological Chemistry, 1983. **258**(15): p. 9536-43.
27. Goto, T. and J.C. Wang, *Yeast DNA topoisomerase II. An ATP-dependent type II topoisomerase that catalyzes the catenation, decatenation, unknotting, and relaxation of double-stranded DNA rings.* Journal of Biological Chemistry, 1982. **257**(10): p. 5866-5872.
28. Mason, T.G., et al., *Particle Tracking Microrheology of Complex Fluids.* Physical Review Letters, 1997. **79**(17): p. 3282-3285.
29. Savin, T. and P.S. Doyle, *Static and Dynamic Errors in Particle Tracking Microrheology.* Biophysical journal, 2005. **88**(1): p. 623-638.
30. Adolf, D. and J.E. Martin, *Time-cure superposition during crosslinking.* Macromolecules, 1990. **23**(15): p. 3700-3704.

31. Larsen, T.H. and E.M. Furst, *Microrheology of the Liquid-Solid Transition during Gelation.* Physical Review Letters, 2008. **100**(14): p. 1460014
32. Larsen, T., K. Schultz, and E.M. Furst, *Hydrogel microrheology near the liquid-solid transition.* Korea-Australia Rheology Journal, 2008. **20**(3): p. 165-173.
33. Corrigan, A.M. and A.M. Donald, *Passive Microrheology of Solvent-Induced Fibrillar Protein Networks†.* Langmuir, 2009. **25**(15): p. 8599-8605.
34. Kundukad, B. and J.R.C. van der Maarel, *Control of the Flow Properties of DNA by Topoisomerase II and Its Targeting Inhibitor.* Biophysical journal, 2010. **99**(6): p. 1906-1915.
35. Zhu, X., B. Kundukad, and J.R.C.v.d. Maarel, *Viscoelasticity of entangled ?-phage DNA solutions*. Vol. 129. 2008: AIP. 185103.

국문 초록

제 II형 토포이소머라아제 (TOP2)는 염색체의 복제, 전사, 복원 등에 관여하는 필수적인 단백질이다. TOP2는 ATP의 수소분해에 의해 에너지를 얻어서 염색체의 엉킴을 풀어주는 역할을 한다. 이 과정은 세포분열의 후반에 결정적인 역할을 하기 때문에 TOP2를 효과적으로 제어하는 것이 오래 전부터 항암제 연구의 화두가 되어왔다.

본 연구에서는 TOP2의 억제제가 원형 염색체 용액의 유변학적 특성에 어떤 변화를 가져오는지에 대해 미세유변학적 관점에서 해석하였다. TOP2의 억제는 모델 억제제인 ATP-PNP와 항암제인 ICRF-193을 적용하였다. TOP2와 염색체의 혼합용액의 유변물성이 억제제에 의해 저점도 용액에서 젤까지 변화하는 양상을 추적입자의 브라운 운동을 관찰함으로써 정량적으로 분석할 수 있었다. TOP2-염색체 젤을 시간-회복 중첩법을 이용하여 미세유변학적 관점에서 매우 정확히 해석할 수 있었다. 이 결과 젤이 되는 순간의 중요지수와 젤이 되는데 걸리는 시간 모두 단백질의 농도가 증가함에 따라 감소하는 것을 관찰하였다.

또한 ICRF-193의 억제 메카니즘이 모델억제제인 AMP-PNP의 억제 메카니즘과 비슷하다는 것을 밝혀 내었다. 이러한 결과는 미세유변학적 해석이 항암제의 스크리닝을 보다 효과적으로 수행 가능하게 하여 항암제 연구개발에 적용 가능함을 보여주었다.

감사의 글

감사하는 마음은 한 없이 큰데 이를 어떻게 표현해야 할지 몰라서 이 감사의 글은 몹시 더디게 운을 떼었습니다. 제 진실된 마음이 모든 분들께 전해지길 기도하며 심호흡 한번 크게 하고 써내려 갑니다.

먼저 학부 1학년 때부터 지금까지 만 7년이 넘는 시간 동안 저를 애정과 관심으로 이끌어 주신 안경현 교수님께 무한한 감사를 드립니다. 방향없이 이리저리 흔들리던 저를 다잡아주시고 큰 사람이 되어 사회에 기여하고자 하는 사명감 또한 갖게 해 주심에 평생의 은인으로 생각하고 있습니다. 그 동안 제게 주신 여러가지 크고 작은 기회들이 저를 단련시키고 여기까지 성장시켰으며 이는 저의 앞날에도 크나큰 재산이 될 것입니다. 교수님께서는 지식인이 어떻게 이 사회를 이롭게 할 수 있는지 몸소 보여주시어 제자로서 한없는 존경과 감동을 품게 하셨습니다. 저 또한 가르쳐 주신대로 사회에 기여할 것을 약속드리며 교수님이 제게 주신 크신 사랑에 조금이나마 보답하겠습니다.

연구실의 큰 어르신 이승종 교수님께도 감사를 드립니다. 교수님의 학문과 세상에 대한 순수한 열정을 존경합니다. 앞으로 교수님이 공부하셨던 곳으로 가게 되어 영광으로 생각하고 있습니다. 아울러 학위심사를 맡아주신 차국헌 교수님과 신규순 교수님께 깊이 감사를 드립니다.

제가 8개월간 싱가폴로 파견 나갔을 때 지도해주신 Patrick S. Doyle 교수님과 Johan van der Maarel 교수님께 감사를 드립니다. 두

분과 함께한 시간은 제 인생에 달콤한 꿈과 같은 순간들이었고 짧은 기간 동안이나마 다채로운 연구의 즐거움을 맛볼 수 있었습니다.

그리고 우리 미세유변학연구실 선, 후배 분들께 감사의 마음을 전합니다. 그 동안 함께 지내면서 제게 잊지 못할 추억을 선물해주셨으며 학문적, 생활적인 모든 측면에서 많은 가르침을 주심에 감사드립니다. 이렇게 좋은 분들을 만나서 참으로 행운이었다고 생각합니다. 이 글에 일일이 이름을 불러드리지 못한 것을 용서하세요. 하지만 한분한분 진정한 마음으로 감사드리며, 제가 마음 깊이 그리워 하고 있다는 것을 알아주셨으면 하는 바람입니다. 떠나는 길이 못내 아쉽지만 앞으로 인연이 또 닿을 것을 믿습니다.

마지막으로 생각만으로도 마음이 따뜻하고 든든해지는 저의 가족에게 감사의 인사를 드리고 싶습니다. 항상 저를 믿어주시고 응원해주시는 아버지! 어머니! 깊이 존경하고 사랑합니다. 제게 있어 세상에서 가장 소중한, 언니 이상의 존재인 울언니에게 한없는 사랑과 깊은 포옹을 전합니다.